

ARTICLE

Location of menaquinone and menaquinol headgroups in model membranes

Cameron Van Cleave, Heide A. Murakami, Nuttaporn Samart, Jordan T. Koehn, Pablo Maldonado, Jr., Heidi D. Kreckel, Elana J. Cope, Andrea Basile, Dean C. Crick, and Debbie C. Crans

Abstract: Menaquinones are lipoquinones that consist of a headgroup (naphthoquinone, menadione) and an isoprenyl sidechain. They function as electron transporters in prokaryotes such as *Mycobacterium tuberculosis*. For these studies, we used Langmuir monolayers and microemulsions to investigate how the menaquinone headgroup (menadione) and the menahydroquinone headgroup (menadiol) interact with model membrane interfaces to determine if differences are observed in the location of these headgroups in a membrane. It has been suggested that the differences in the locations are mainly caused by the isoprenyl sidechain rather than the headgroup quinone-to-quinol reduction during electron transport. This study presents evidence that suggests the influence of the headgroup drives the movement of the oxidized quinone and the reduced hydroquinone to different locations within the interface. Utilizing the model membranes of microemulsions and Langmuir monolayers, it is determined whether or not there is a difference in the location of menadione and menadiol within the interface. Based on our findings, we conclude that the menadione and menadiol may reside in different locations within model membranes. It follows that if menaquinone moves within the cell membrane upon menaquinol formation, it is due at least in part, to the differences in the properties of headgroup interactions with the membrane in addition to the isoprenyl sidechain.

Key words: menaquinone, menadione, menadiol, Langmuir monolayer, reverse micelle.

Résumé: Les ménaquinones sont des lipoquinones formées d'un groupement de tête (naphtoquinone, ménadione) et d'une chaîne latérale isoprényle. Elles servent de transporteurs d'électrons dans les procaryotes tels que Mycobacterium tuberculosis. Dans le cadre des présents travaux, nous avons employé des monocouches de Langmuir et des microémulsions pour étudier la manière dont le groupement de tête de la ménaquinone (la ménadione) et le groupement de tête de la ménahydroquinone (le ménadiol) interagissent avec les interfaces du modèle membranaire. Cette étude avait pour but de déterminer si des différences peuvent être décelées quant aux endroits où ces groupements de tête se situent à l'intérieur d'une membrane. L'hypothèse selon laquelle ces différences de position seraient essentiellement attribuables à la chaîne latérale plutôt qu'à la réduction de la quinone en quinol durant le transport d'électrons a été posée. Cette étude présente des éléments qui tendent à démontrer que la quinone oxydée et l'hydroquinone réduite se déplacent à des endroits différents dans la membrane cellulaire, et ce, sans influence de la chaîne latérale. À l'aide de membranes modèles de microémulsions et de monocouches de Langmuir, nous avons pu déterminer s'il y avait ou non une différence de position entre la ménadione et le ménadiol dans la membrane. Nos résultats ont permis de conclure que la ménadione et le ménadiol peuvent se situer à des endroits différents dans les membranes modèles. Par conséquent, si la ménaquinone se déplace dans la membrane cellulaire lorsqu'elle se transforme en ménaquinol, ce déplacement est attribuable non seulement à la chaîne isoprényle, mais aussi, du moins en partie, à la différence des propriétés des interactions entre le groupement de tête et la membrane. [Traduit par la Rédaction]

Mots-clés: ménaquinone, ménadione, ménadiol, monocouche de Langmuir, micelle inversée.

1. Introduction

Lipoquinones are an essential group of lipids that act as electron transfer donors and acceptors within the electron transfer complex.^{1,2} One type of lipoquinone typically associated with prokaryotes is menaquinone (MK), which has a naphthoquinone headgroup, as well as an isoprenyl sidechain.^{3–6} The menaquinone abbreviations are based on the naphthoquinone headgroup

and the number of isoprene groups in the sidechain, where MK-4 is a menaquinone with four isoprene units. Some of the MK derivatives are known to have biological activities in humans such as MK-4, which is important in blood coagulation. Other MK analogs have been reported to have potent biological properties such as antiseizure activity in model organisms. Other activity electron transport lipoquinone of Mycobacterium spp., specifically M is M is M in M in M in M is M in M is M in M i

Received 15 January 2020. Accepted 30 March 2020.

C. Van Cleave, H.A. Murakami, J.T. Koehn, P. Maldonado, Jr., H.D. Kreckel, E.J. Cope, and A. Basile. Department of Chemistry, Colorado State University, Fort Collins, CO 80523, USA.

N. Samart. Department of Chemistry, Colorado State University, Fort Collins, CO 80523, USA; Department of Chemistry, Rajabhat Rajanagarindra University, Chachoengsao, Thailand.

D.C. Crick. Cell and Molecular Biology Program, Colorado State University, Fort Collins, CO 80523, USA; Department of Microbiology, Immunology, and Pathology, Colorado State University, Fort Collins, CO 80523, USA.

D.C. Crans. Department of Chemistry, Colorado State University, Fort Collins, CO 80523, USA; Cell and Molecular Biology Program, Colorado State University, Fort Collins, CO 80523, USA.

Corresponding author: Debbie Crans (email: debbie.crans@colostate.edu).

This paper is part of a special issue to honour Professor Jim Wuest.

Copyright remains with the author(s) or their institution(s). Permission for reuse (free in most cases) can be obtained from RightsLink.

Fig. 1. Structures for (A) menaquinone (MK-9(II-H₂)) present in M. tuberculosis, (B) the oxidized headgroup menadione (MEN), and (C) the reduced headgroup menadiol (MDL).

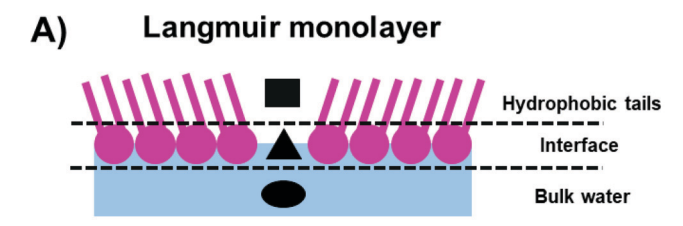
C) Menadiol (MDL) $H_{c} \xrightarrow{H_{d'}} OH_{v} H_{e'}$ $H_{d'} \longrightarrow OH_{w}$

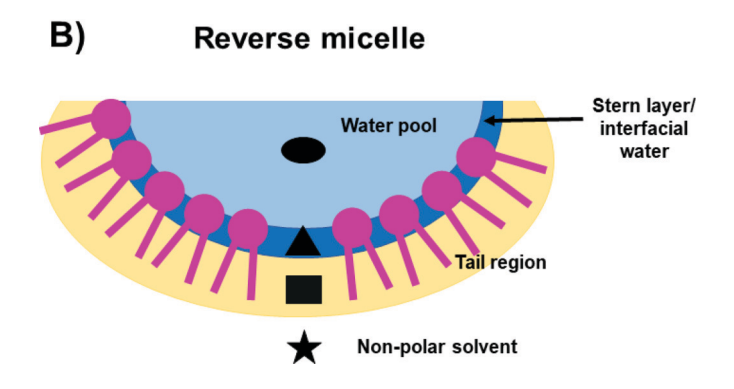
viated as MK-9(II-H₂), Fig. 1A). ^{11,12} The electron transfer complexes of most organisms are membrane associated and thus require that the MK derivatives are also affiliated with the membrane. Native prokaryotic MKs have long isoprenyl sidechains and their native conformations are poorly understood. Their hydrophobic nature and insolubility in aqueous assays complicates analyses of these molecules. ⁶ Considering the challenges of working with the native systems, we have initiated studies with truncated MK derivatives that are slightly water soluble. ^{1,6,13} Their simpler and less hydrophobic structures allow for characterization of how these MK systems interact with membrane interfaces and elucidation of their conformations. ^{6,13} We have recently shown that the truncated MK-1 and MK-2 molecules fold and that such folding adjusts as the molecule associates with a model membrane interface. ^{1,13}

The MK derivatives are reduced by the electron transfer complex to form their quinol counterparts. Reduced MKs are suggested to interact differently with the interface compared with oxidized MKs, based on computational and experimental studies on MK's counterpart, ubiquinone.14-16 In this manuscript, we sought to obtain experimental evidence investigating whether the interaction with interfaces differs between the oxidized menadione (MEN) and reduced menadiol (MDL) headgroups. Previous studies of the MK derivatives with interfaces take advantage of work with two model interface systems, Langmuir monolayers^{17,18} and microemulsions.^{19,20} Generalized diagrams of both model membranes and potential locations of probe molecules are shown in Fig. 2. Studies using Langmuir monolayer systems with truncated MK derivatives have been reported and support the interpretation that the MK derivatives insert into the membrane interface. 1,21 The studies with microemulsions were carried out using a well-known model system for studying membrane interface interactions, consisting of a lipid or surfactant (aerosol-OT, abbreviated AOT), an organic solvent (isooctane), and water. 22-24 This system forms self-assembled structures with an interface resembling that of a charged membrane,19,25-27 making it a very useful tool for studying the interactions and potential penetration of naphthoquinone and naphthoquinol headgroups. 13,18 Both models have been used successfully in conjunction with each other to develop a more in-depth framework of how different biologically relevant molecules interact with the cell membrane. 28,29

Computational analysis and other studies have been carried out, which suggest that the interactions of MK and ubiquinone derivatives within the membrane are dictated mainly by the length of the isoprene sidechain.³⁰ In other studies in neutral bilayers, the naphthoquinone headgroup was important for anchoring the lipoquinone, suggesting that the isoprene may not be the only structural factor determining the location in the membrane.^{14,31} Anchoring through a headgroup has been noted with other molecules as well.^{32,33} In the following work, we examined

Fig. 2. General diagrams of (A) a Langmuir monolayer and (B) a reverse micelle (RM) microemulsion. Black rectangles represent probe molecules found in the hydrophobic tails, black triangles represent molecules found in the interface, black ovals represent molecules found in the bulk water, and black stars represent molecules found in the non-polar solvent of the RM system. [Colour online.]





the interaction of the headgroup, MEN (Fig. 1A), and the corresponding reduced version, MDL (Fig. 1C), with a model membrane interface. We hypothesize that the headgroup will interact and penetrate into the membrane but that there are differences in how MEN and MDL interact with the interface. These studies are important and provide experimental evidence for the role of the headgroup in the interaction of the MK derivatives at the cell membrane interface.

2. Materials and methods

2.1. General materials and methods

2.1.1 Materials

MEN was purchased from Sigma-Aldrich. MDL was prepared as reported previously. 1,34 Chloroform (\geq 99.5%), dithiothreitol (DTT), monosodium phosphate (\geq 99.0%), disodium phosphate (\geq 99.0%), sodium hydroxide (\geq 98%), hydrochloric acid (37%), and MEN were all purchased from Sigma-Aldrich. Dipalmitoylphosphatidylcholine

(DPPC, ≥99%) and dipalmitoylphosphatidylethanolamine (DPPE, 99%) were purchased from Avanti Polar Lipids. Most materials were used without further purification. AOT (Sigma-Aldrich) was purified using charcoal and methanol as described previously. The water content of the AOT was determined by NMR spectroscopy, measuring the water content in AOT solubilized in DMSO. Distilled deionized (DDI) water was obtained by filtering distilled water through a water purification system, obtaining a resistance of 18.2 MΩ.

2.1.2. Instrumentation

All absorption spectra were run on an Avantes spectrophotometer (AvaSpec-USB2 with an AvaLight-DHc lamp) in 1 cm quartz cuvettes and collected with AfterMath software version 1.4.7881. The Langmuir monolayers were studied using a NIMA LB Medium Trough (Teflon) from Biolin Scientific. NMR studies were conducted on a Bruker Neo400 NMR. Dynamic light scattering (DLS) studies were performed in a Malvern Zetasizer Nano ZS equipped with a 633 nm red laser.

2.2. Synthesis of MDL

MDL was synthesized by the reduction of MEN by sodium dithionite, and NMR spectra of MDL were consistent with those reported previously.^{1,34}

2.3. Stability studies with UV-vis spectroscopy

Because of the limited solubility of the oxidized and reduced headgroups, as well as the rapid oxidation of the reduced headgroup, a number of different methods were investigated for preparation of the solutions. Attempts to sonicate the samples under argon were not as effective as the addition of a reductant of MDL samples.

2.3.1. Stability in DDI water

A solution of 0.10 mmol/L MEN (yellow powder) was made by sonicating 17 mg (10 μmol) of MEN in 100 mL of DDI water (18.2 M Ω) until dissolved, approximately 10 min. A solution of 0.10 mmol/L MDL (pale purple powder) was made by sonicating 17 mg (10 μmol) of MDL in 100 mmol/L of DDI water for approximately 20 min. A third sample was prepared by adding 17 mg of MDL (10 μmol) to 100 mL of DDI water, shaking for five seconds, and removing the supernatant to observe the spectra of MDL immediately after contact with water. A fourth sample was prepared by adding a small amount of solid MDL to the bottom of a cuvette and then adding water. Spectra were collected every minute for 15 min and then at the 20, 25, 30, 45, and 60 minute marks. Although one may have anticipated that MDL would be more soluble than MEN because of the two hydroxyl groups, the fact that the MDL takes longer to dissolve than MEN is not consistent with this observation. Although hydroxyl groups typically increase solubility, this is not always the case. For example, the [VO₂(dipic-OH)]⁻ complex is less soluble than the parent complex, [VO₂dipic]⁻ complex, possibly because the former imparts greater solid-state interactions, which decrease the solubility.36

2.3.2. Stability in DDI water with a reducing agent

DTT was used to create a reducing environment to test for an improvement in MDL stability. Due to the rapid oxidation of MDL in water, a small amount of MDL solid was added to the bottom of a quartz cuvette with a small amount of DTT. DDI water was added and a UV-vis spectrum was recorded immediately. Timepoints were taken with the same frequency as described in the previous section.

2.3.3. Stability of MDL in a reverse micelle microemulsion

A stock solution of w_0 12, AOT/isooctane reverse micelles was prepared by mixing appropriate amounts of 0.50 mol/L AOT in isooctane with DDI water and agitating for 30 s until the solution became translucent. The sample for UV–vis was prepared by dilut-

ing 1.0 mL of the stock solution into 4.0 mL of isooctane and agitating for 2 min to break up aggregates. Approximately 1.0 mL of the dilution was added to a cuvette with solid MDL and immediately placed into the UV–vis spectrophotometer (t = 0). The same timepoints were collected as described in the previous sections.

2.4. Preparation of solutions for Langmuir monolayers studies

2.4.1. Phospholipid and menaquinone stock solutions

Phospholipid stock solutions were prepared by dissolving dipalmitoylphosphatidylcholine (DPPC) (0.018 g, 0.025 mmol) or dipalmitoylphosphatidylethanolamine (DPPE) (0.017 g, 0.025 mmol) in 25 mL of 9:1 chloroform/methanol (ν/ν) for a final concentration of 1.0 mmol/L phospholipid. MEN stock solutions were prepared by dissolving MEN (0.0043 g, 0.025 mmol) in 25 mL of 9:1 chloroform/methanol (ν/ν) for a final concentration of 1.0 mmol/L MEN. Solutions with ratios of 50:50 and 25:75 (phospholipid/MEN) were prepared in 2.0 mL glass vials and vortexed for 10 s before each experiment.

2.5. Langmuir monolayers studies

2.5.1. Preparation of phospholipid Langmuir monolayers

The aqueous subphase consisted of 230 mL of 20 mmol/L sodium phosphate buffer (pH 7.4) in DDI water (18.2 M Ω). The subphase surface was cleaned using vacuum aspiration, and the surface pressure of a compression isotherm of just the subphase (no phospholipid present) was measured (surface pressure was consistently 0.0 ± 0.5 mN/m throughout compression) before each compression measurement. To prepare the DPPC phospholipid monolayer, a total of 28 μ L of phospholipid stock solution (28 ng of DPPC) was added to the surface of the subphase in a dropwise manner using a 50 μ L Hamilton syringe approximately 1 inch from each expanded barrier. The film was allowed to equilibrate for 15 min during which time the chloroform and methanol evaporated. The resulting phospholipid monolayer was then used for the compression isotherm experiments.

The preparation of the Langmuir monolayer from DPPE phospholipids required a higher lipid amount and the injection volume of 58 μ L was compared with the DPPC solution. Solutions with ratios of 50:50, and 25:75 (phospholipid/MEN) shared the base injection volume of phospholipid plus an appropriate amount of MEN to reach the desired ratio of phospholipid/MEN.

2.5.2. Compression isotherm surface pressure measurements of Langmuir monolayers

The phospholipid monolayer was compressed from two sides with a total speed of 10 mm/min (5 mm/min from opposite sides) using a NIMA LB Medium Trough from Biolin Scientific. The temperature was maintained at 25 °C using an external water bath. The trough base and Teflon barriers were rinsed three times with ethanol followed by DDI water (18.2 $\mathrm{M}\Omega$) before each experiment. The surface tension of the subphase during each compression was monitored using a platinum Wilhemy plate. The surface pressure was calculated from the surface tension using eq. 1, where π is the surface pressure, γ_{o} is the surface tension of water (72.8 mN/m), and γ is the surface tension at a given area per phospholipid after the film has been applied.

(1)
$$\pi = \gamma_o - \gamma$$

The compression moduli were calculated and are shown as detailed in the Supplementary data. Each compression isotherm experiment consisted of at least three replicates, and the averages of the area per phospholipid and the standard deviation at every 5 mN/m were calculated using Microsoft Excel. The areas of the mixed monolayers were multiplied by the mol fraction to plot curves in terms of area per phospholipid as opposed to area per

molecule. This allowed for easier comparison with the control. The worked-up data were transferred to OriginPro version 9.1 to be graphed showing the variation in the measurements.

2.6. Reverse micelle (RM) solutions in AOT/isooctane

2.6.1. MEN

Because MEN was sparingly soluble in $\rm H_2O$ (or $\rm D_2O$) the AOT/ isooctane RM samples were prepared by dissolving MEN directly into a mixture of AOT in isooctane followed by the addition of $\rm D_2O$. A 0.5 mol/L stock solution of AOT in isooctane was prepared by dissolving 5.56 g, 12.5 mmol AOT in 25 mL isooctane. To prepare a 14.3 mmol/L MEN solution, 0.6 g of MEN was added to a 25 mL volumetric flask followed by the AOT/isooctane stock solution. The mixture was sonicated until MEN was fully dissolved and then diluted to the mark. The pH of a $\rm D_2O$ solution was adjusted to 7.0 (pD = pH + 0.4). To 2 mL of the MEN/AOT/isooctane stock of solution varying amounts of pH adjusted $\rm D_2O$ was added to prepare samples with w_0 4, w_0 8, w_0 12, w_0 16, and w_0 20 for MEN. These samples were vortexed until clear, indicating that the microemulsions were formed.

2.6.2. MDL

As in the case of solution preparation for studies by UV-vis spectroscopy, several methods were investigated to prepare the higher concentration solutions for NMR investigations including use of different solvents and solvent mixtures, as well as mixed solid systems, and the addition of the RM mixture into an NMR tube containing the solid at the bottom. Due to the rapid oxidation of MDL to MEN, methanol was added to the "water pool" of the RMs to both solubilize and stabilize MDL against oxidation. The mixed solvent MeOH/D2O samples were prepared similarly to the D₂O samples in a 10 mL volumetric flask adding first MeOH (7.0, 8.0, and 9.0 mL) followed by D₂O to make up the 10 mL volume (note that MeOH/D2O decrease volume when combined, so the values reported here overestimate the MeOH content). Several mixed solvent pools were made but only the 70:30, 80:20, and 90:10 mixtures were able to dissolve MDL. After vortexing, the mixed solvents were used to prepare samples as described above $(0.20 \text{ mg/}1.15 \mu\text{mol in } 1.00 \text{ mL mixed solvents})$. As MDL was poorly soluble in aqueous and D₂O solutions, solid MDL was added to the NMR tube prior to AOT/isooctane RM solution. Specifically, microemulsion solutions for NMR studies were prepared by the addition of 0.20 mg (1.2 µmol) MDL to the tube followed by 1 mL of AOT/isooctane RM solution. This experiment corresponded to the addition of solid MDL to an "empty" RM. NMR spectra were collected immediately.

2.6.3. ¹H NMR spectroscopic studies of AOT/isooctane RM samples

One-dimensional (1D) 1 H NMR spectra of MEN and MDL in D_2O , organic solvent, and RMs. Two-dimensional (2D) 1 H NMR studies of MEN and MDL were carried out in organic solvent and in RMs as reported previously. 20 The parameters to record the NOESY and ROESY spectra were recorded using parameters reported previously. 1

2.7. Dynamic light scattering (DLS) studies

DLS samples were prepared similar to the RM NMR samples described above but with the following modifications: DI water was used in place of $\rm D_2O$, and once the 1 mL sample was made, 4 mL of isooctane were added to dilute the sample. Diluted samples were agitated for 2 min prior to measurements to break up RM aggregates.

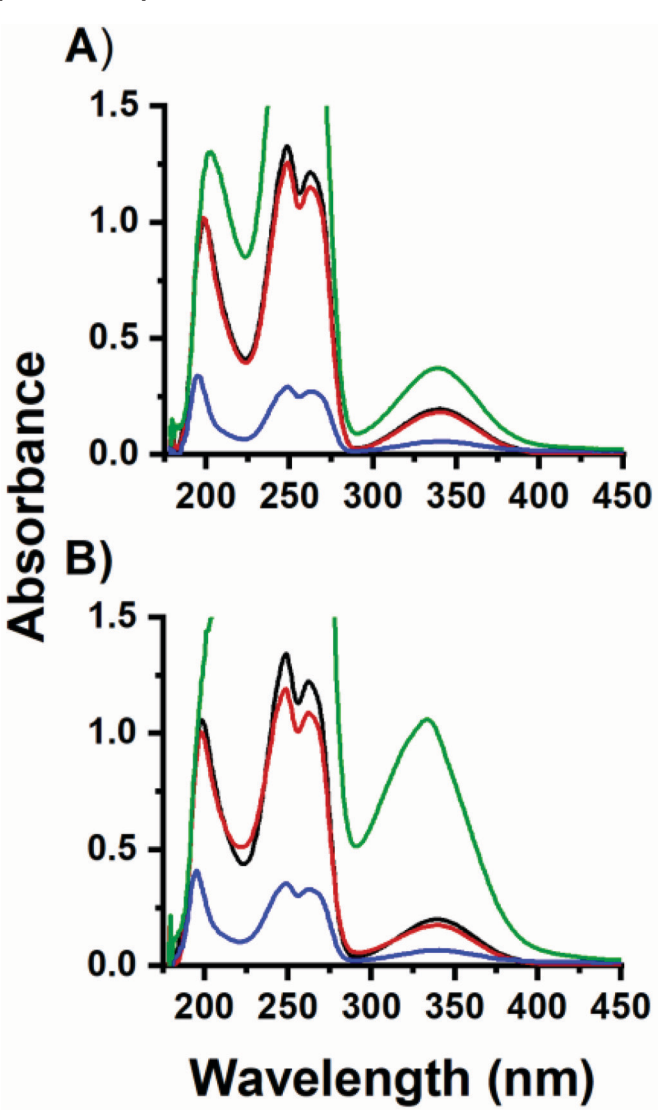
3. Results

3.1. Stability of MEN and MDL in aqueous solution

3.1.1. MEN and MDL in aqueous solution

MEN is stable in aqueous solution albeit sparingly soluble, requiring agitation or sonication for dissolution. MDL, on the other

Fig. 3. Aqueous UV–vis spectra of 0.10 mmol/L MEN (black), 0.10 mmol/L MDL that was fully dissolved before analysis (red), supernatant from a 0.1 mmol/L MDL solution when MDL had just been added to water (blue), and aqueous solution added to solid MDL at the bottom of the quartz cuvette (green). Spectra are shown at times (A) t=0 min and (B) t=60 min after dissolution of the MDL material. The y axis is cut off at 1.5 as any peaks above that value in the absorbance spectrum are associated with high experimental uncertainly. Full spectra are provided in Supplementary Fig. S2. [Colour online.]



hand, oxidizes to MEN, so stability studies in water were conducted to determine the time that the reaction takes place to define the parameters of the experimental design. Several different approaches to sample preparation for MDL were tested against MEN with UV–vis spectroscopy. These consisted of dissolving MDL completely in water, taking an aliquot of supernatant from a fresh mixture of MDL and water, and placing solid MDL at the bottom of a vessel such as a cuvette. The potential to carry out MDL solution preparation under argon was considered but not pursued because of the difficulties in dissolving the compound in a timely manner.

The absorption spectrum shown in Fig. 3 of 0.1 mmol/L MEN contains four peaks that appear at 198 nm, 248 nm, 263 nm, and 339 nm. This solution was found to be stable over 60 min (see Supplementary Fig. S1). The UV–vis spectra of the 0.1 mmol/L MDL

sample prepared by sonication has four peaks at 198 nm, 248 nm, 261 nm, and 341 nm, which is identical to that observed for MEN and thus documents complete oxidation by the time the solid MDL had dissolved (Fig. 3A). After 60 min, small differences were observed for the signal at 225 nm and the two signals at 248 nm and 263 nm. An aliquot of MDL supernatant taken from a sample where MDL had just been added to water had peaks at 194 nm, 248 nm, 263 nm, and 340 nm but at a lower intensity. Some of these peaks are slightly shifted from pure MEN (Fig. 3). In addition, the peak at 194 nm had a higher intensity than the peaks at 248 nm and 263 nm, which is the opposite spectroscopic signature for dissolved MDL. This suggests that the sample contained something other than MEN.

The sample of solid MDL added directly in a cuvette followed by the addition of water showed the peaks that were present at 203 nm, 249 nm, and 262 nm had coalesced into a single signal with an intensity above an absorbance where the spectrophotometer measured intensities accurately (Fig. 3B). These experiments demonstrate that MDL has limited solubility and it rapidly oxidizes as it dissolves. In a system where solid MDL is present at the bottom of the cuvette, the MDL can continuously dissolve and consequently continuously oxidize. The data shown for both the 0 min and 60 min time points of the MDL sample (Fig. 3) demonstrate that even at t = 0 significantly more than 0.1 mmol/L MDL has been dissolved and oxidized to MEN. As the Langmuir monolayer studies take approximately 45 min for completion, where MDL would be exposed to bulk and interfacial water, such studies would be examinations of MEN as opposed to MDL. Thus, Langmuir monolayer studies were not attempted starting from MDL due to its rapid oxidation. Regardless, the data in Fig. 3B show that the studies performed so far gives a spectrum identical to that of MEN and thus confirmed that MDL oxidized in solutions where it was allowed to fully dissolve in the time it took to prepare the solution. To validate this interpretation, we sought to dissolve MDL under conditions where it remained in the reduced form.

3.1.2. MEN and MDL in reducing aqueous solution

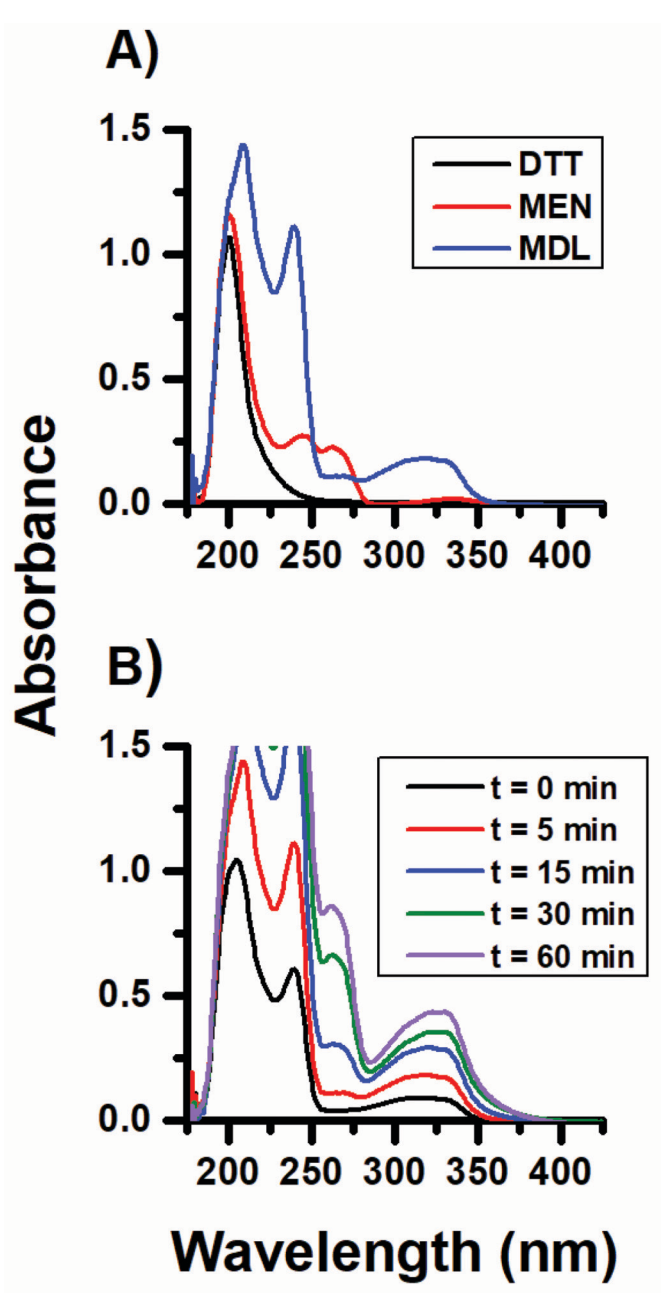
To keep MDL in a reduced form, solid DTT was added to the cuvette alongside solid MDL with the intent to generate a solution with a reducing environment, thus decreasing spontaneous oxidation of MDL. Such a solution should allow for the observation of MDL instead of MEN (Fig. 4). Figure 4B shows that a solution formed from the addition of both MDL (239 nm signal) and DTT followed by the addition of water will begin oxidizing MDL to MEN as evidenced by the 263 nm signal by the 15 min timepoint. A control sample was recorded where solid DTT and MEN were added to the quartz cuvette followed by the addition of water. This experiment verifies the spectrum for MEN by the presence of the 263 nm signal as opposed to the MDL signals and is shown in Fig. 4A.

The use of a reducing agent did decrease the oxidation rate of MDL to MEN, and it was possible to record a spectrum of MDL in the presence of DTT. This verifies that the UV-vis spectrum of MDL is different than that of the MEN. Considering that these spectra were recorded from solid added to the quartz cuvette, the concentrations cannot be accurately determined unlike those shown in Fig. 3, which is why the signal intensity for the MEN is smaller than that observed for MDL. However, it is not appropriate to use such solid mixture in Langmuir monolayer studies due to the exposure to open air and continuous oxidation under those conditions, as well as the potential effects of DTT on the monolayer itself. Accordingly, an alternative model membrane system, microemulsions, was investigated in place of the Langmuir monolayer studies.

3.2. Effects of MEN on DPPE and DPPC monolayers

The effects of MEN on a Langmuir monolayer were investigated using both DPPE and DPPC. These phospholipids were chosen as

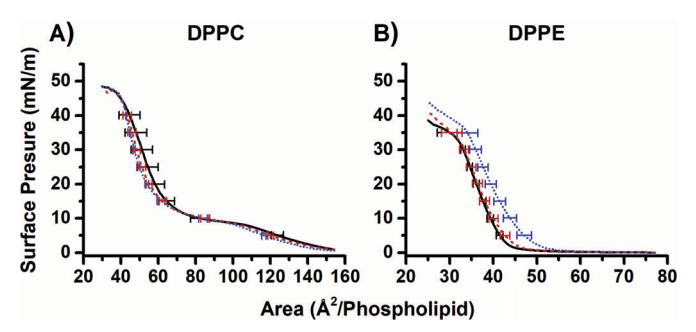
Fig. 4. UV–vis spectra showing (A) a solution of DTT (blue), a solution formed from the addition of solid MEN and DTT (red) in a quartz cuvette followed by the addition of DDI water, and a solution formed from the addition of solid MDL and DTT in a quartz cuvette followed by DDI water (black) and (B) a solution formed by the addition of solid MDL and DTT to a quartz cuvette followed by DDI water as a function of time from the addition of the DDI water at time 0 over 60 min. The *y* axis is truncated to 1.5, as any peaks above that value are associated with high error. [Colour online.]



they have been thoroughly characterized in Langmuir monolayer systems and their biological relevance has also been characterized. DPPC is up to 40% of human lung surfactant, whereas DPPE is commonly found in prokaryotic cell membranes and the inner leaflet of eukaryotic cells.^{37–39}

Although MEN is a hydrophobic molecule, it was unable to form a monolayer on the subphase, even with increasing amounts of MEN. This implies that MEN is either surface inactive, much like

Fig. 5. Compression isotherms of (A) DPPC and (B) DPPE with varying mol fractions of MEN as a function of area per phospholipid. Solid black curves represent DPPC or DPPE controls. Red dashed curves represent 50:50 lipid/MEN monolayers, and dotted blue curves are 25:75 lipid/MEN monolayers. [Colour online.]



geranyl bromide (unpublished data), or that MEN was π – π stacking in the aqueous solution, thus preventing the formation of a film.

As shown in Fig. 5, the DPPC monolayers exhibited the expected gas-liquid transition between 155 and 110 Å² (0-10 mN/m), which is in accordance to the literature for the amount of lipid added.18,37 The 50:50 and 25:75 DPPC/MEN curves exhibit an overall similar shape as the pure DPPC samples, though both are slightly shifted to a smaller area per phospholipid. However, the observed variation in the area measurements overlap with the variation in the control: therefore, we cannot conclude that there is a difference in area. This indicates that MEN is located in either the bulk water or the hydrophobic tail region. Given the sparing solubility of MEN in water, it is more likely that MEN was compressed into the hydrophobic phospholipid tails. This was confirmed by compression modulus calculations shown in Supplementary Fig. S5, where the compression modulus was affected by the presence of MEN in DPPC. These observations are consistent with the insertion of MEN into the monolayer.

The DPPE control curves has a shape and areas that are consistent with what is reported in the literature.³⁷ The curve shifts towards a greater area per phospholipid as the mol fraction of DPPE is decreased while the curve maintains its shape. These results are consistent with the possibility that MEN is located directly at the air–water interface without being compressed up into the phospholipid tails. These results support the report showing that the idebenone/idebenol pair remains at the water–lipid interface,³³ though the physical properties of the lipid or surfactant will have an effect on distribution of the molecule of interest.⁴⁰ To this effect, the physical properties of DPPC and DPPE resulted in different interaction with MEN, which supports that lipid composition of the cell membrane could also affect the location of lipoquinones.

3.3. MEN and MDL in the AOT RM model membrane system

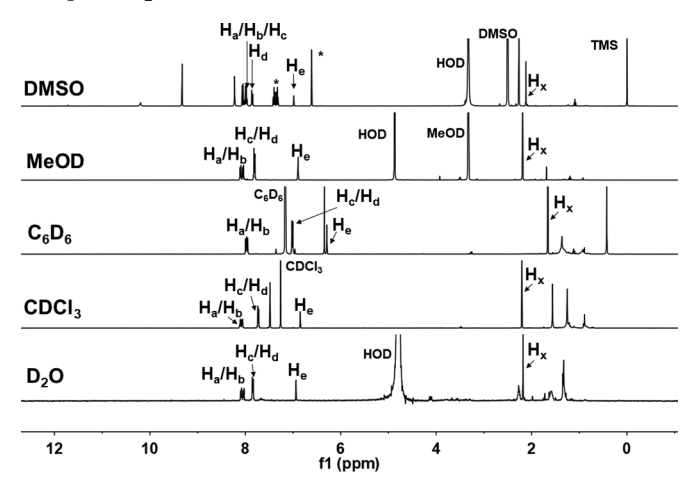
3.3.1. MEN in microemulsions

The solubility of MEN in aqueous solution is limited (albeit higher than MDL's solubility), but enough compound can be dissolved in $\rm D_2O$ that a $\rm ^1H$ NMR spectrum can be recorded after agitating the suspensions (Fig. 6). The aromatic protons are in a chemical shift range well separated from the signals from the RM surfactant with the quinone proton ($\rm H_e$) slightly more upfield than the benzene protons ($\rm H_a-H_d$). The aliphatic methyl group on the quinone unit on the other hand is in the range of the AOT protons around 2.3 ppm. There is a large difference between the $\rm ^1H$ NMR spectrum in $\rm D_2O$ and in an organic solvent such as isooctane, as shown in Fig. 6.

3.3.2. MDL in microemulsions

The ¹H NMR of MDL were recorded in a number of solvents including D₂O, MeOD, d₆-DMSO, d₆-benzene, and CDCl₃, as shown

Fig. 6. ¹H NMR spectra of MEN in d₆-DMSO, MeOD, d₆-benzene, CDCl₃, and D₂O.



in Fig. 7. The oxidation of MDL is visually observed by the colour change of the light purple MDL to the yellow MEN. Complete dissolution of MDL in D₂O, d₆-benzene, and CDCl₃ required incubation overnight or sonication and agitation. As a result, for the MDL samples in d₆-benzene, D₂O, and CDCl₃, the NMR solvent was added to solid MDL in the NMR tube and the ¹H NMR spectra were collected immediately. Although the rate of MDL oxidation was dependent on the solvent, the oxidation was found to be rapid in all solvents. Although some amount of the solid MDL samples was suspended in the NMR tube when the NMR spectrum was being recorded, the time it would take to dissolve the MDL sample fully would have caused significant or complete oxidation. The NMR results shown in Fig. 7 indicate that the MDL was present in all solvents tested regardless of the low solubility of the MDL. The ¹H NMR spectra of MDL show five protons in the aromatic region, with the proton on the hydroquinone group being more than 1 ppm upfield from the other aromatic protons and the aliphatic protons around 2.3 ppm. The proton most different between the MEN and MDL is the proton on the quinone or the hydroquinone, H_e. However, even by recording the sample immediately after adding deuterated solvent to the NMR tube led to formation of some MEN in the samples, indicated by the * in the spectra for MDL shown in Fig. 7.

MDL was very soluble in d_6 -DMSO and MeOD. As shown in Fig. 8, the MDL oxidized less rapidly in d_6 -DMSO and the data for d_6 -benzene, CDCl $_3$, and D $_2$ O are given in the Supplementary data. As illustrated in Fig. 7, it was possible to obtain spectra of not only the MDL but also the MEN that is formed in these solvents, and we show the spectra as a function of time. 1 H NMR spectra performed as a function of time in MeOD showed that the reduced MDL existed for about 1 h (Fig. 8). Considering that microemulsions have been reported with "water pools" containing methanol, it was possible to record spectra of MDL in AOT reverse micelles with MeOH-containing "water pools". 41,42

3.3.3. Stability of MDL in RM samples

UV–vis spectra of MDL in w_0 12 RMs were collected to assess oxidation of MDL to MEN in the RM system. As with the aqueous samples described in the above stability section, MDL was found to start oxidizing with the first 15 min of exposure to the solution, as shown in Fig. 9. The characteristic MEN peak at 263 nm begins to appear by the fifth minute, confirming the NMR studies above in the need for a mixed solvent "water pool" to increase stability.

Fig. 7. 1 H NMR spectra of MDL in d_{6} -DMSO, MeOD, d_{6} -benzene, CDCl $_{3}$, and D_{2} O. The signals for MEN beginning to form in these spectra are labeled with an asterisk (*).

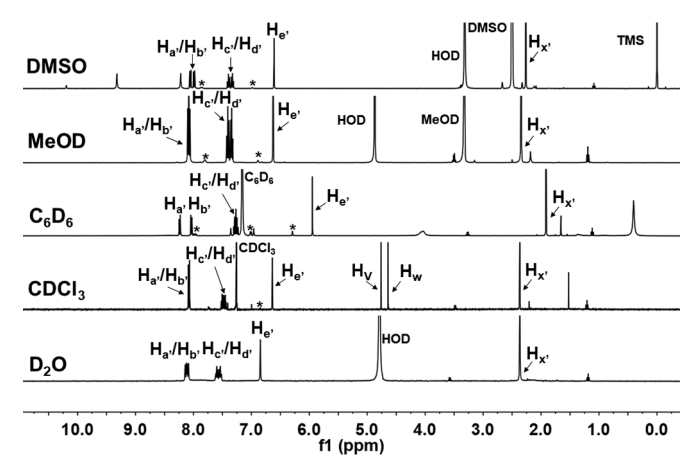
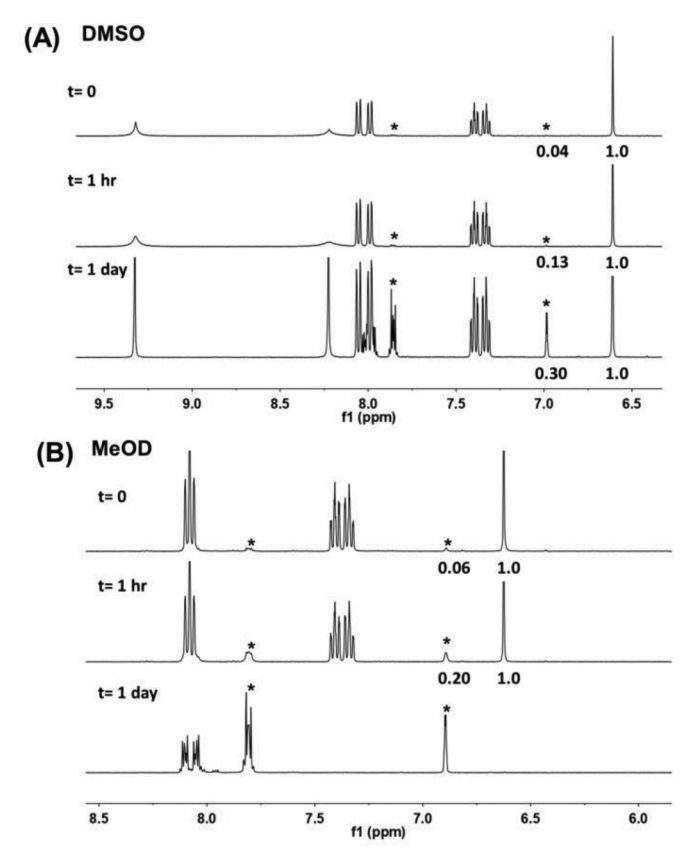


Fig. 8. Spectra recorded of MDL as a function of time in solvents where it is readily soluble such as (A) d₆-DMSO and (B) MeOD. The increase in the ¹H NMR signals are due to formation of MEN and these signals are indicated by an asterisk (*).



3.4. Interactions of MEN and MDL in AOT/isooctane RM samples

3.4.1. MEN in microemulsions

 1 H NMR spectra were recorded in 0.50 mol/L AOT/isooctane to investigate the interactions of MEN with another type of model membrane interface. The w_0 sizes were varied from w_0 4 to w_0 20. The 1D 1 H NMR spectra show that the chemical shifts for MEN were very different from those observed in isooctane and in D_2O (Fig. 10). The chemical shifts change for H_a was less than 0.1 ppm,

Fig. 9. UV–vis spectra of solid MDL dissolving into a w_0 12 RM solution (0.5 mol/L AOT in isooctane) in 1 min increments over 15 min. The peak for the MDL (239 nm) increases rapidly until about 15 min, at which point a significant amount of both MDL and MEN (263 nm) have formed and the accuracy of the UV–vis spectra begins to decrease due to experimental error. [Colour online.]

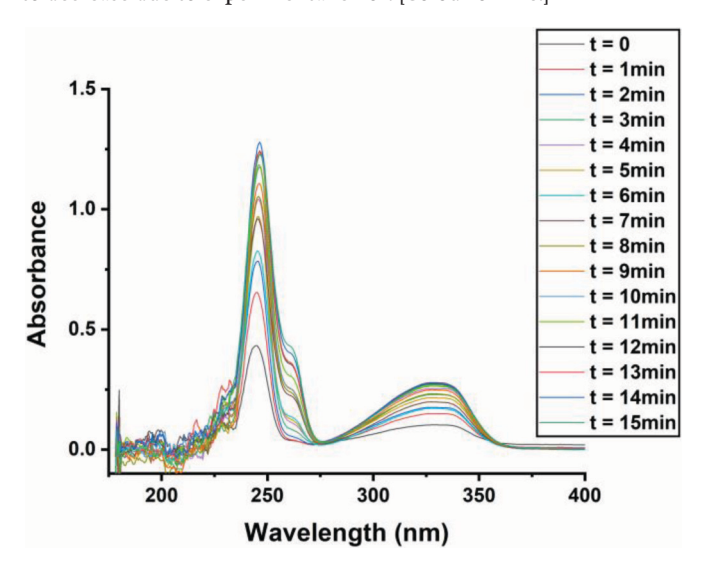
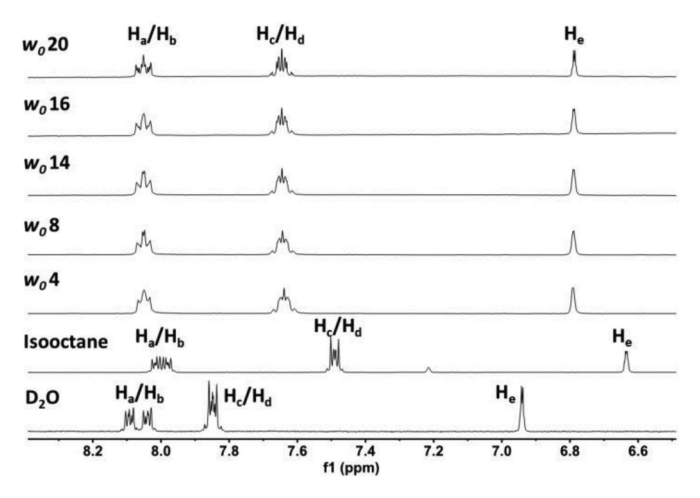


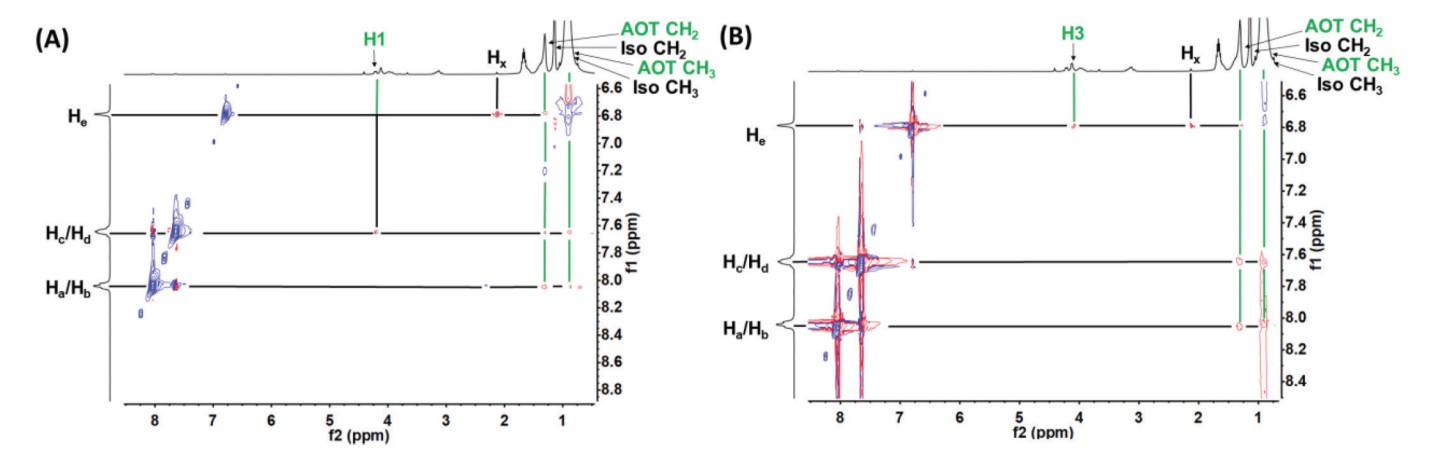
Fig. 10. Partial ¹H NMR spectra of MEN in AOT/isooctane RM ranging from w_0 from 4 to 20. The ¹H NMR spectra of MEN in D_2O and in isooctane are shown for comparison and demonstrate that the AOT/isooctane RM environment of the MEN is very different depending on proximity to a solvent.



whereas the shifting was 0.2 ppm for $\rm H_b$ and about 0.3 ppm as the quinone proton. These shifts show that MEN resides in neither the aqueous environment of the water pool, nor the organic isooctane solution, consistent with placement in the interface of the AOT RM.

2D NMR spectra including NOESY and ROESY spectra (see Supplementary data) were recorded for the MEN in RM samples and the partial spectra are shown in Fig. 11. These spectra showed that proton H_e correlates to H_x , which serves as an internal control. Weak signals between H_a/H_b , H_c/H_d , and H_e with AOT protons H_1 and H_3 and part of the AOT CH_2 and CH_3 tail groups (H5-H10, H5'-H10', see Supplementary data for AOT labeling key) show that the placement of the MEN can vary from the headgroup to farther up in the tail region. Further investigation into whether similar conclusions could be reached with the MDL system led to the following NMR experiments.

Fig. 11. Partial 1 H- 1 H 2D (A) NOESY and (B) ROESY NMR (400 MHz) spectra of MEN inside w_0 12 RM at 26 $^{\circ}$ C. Blue intensity contours represented negative NOEs or ROEs and red intensity contours represent positive NOEs or ROEs. A standard NOESY pulse consisted of 256 transients with 16 scans in the f_1 domain using a 200 ms mixing time and a 1.5 s relaxation delay. A standard ROESYAD pulse consisted of 256 transients with 16 scans in the f_1 domain using a 200 ms mixing time and a 2.0 s relaxation delay. Green lines indicate MEN proton interactions with AOT protons. [Colour online.]



3.4.2. MDL in microemulsions

Given the insolubility and instability of MDL in D₂O, an alternative co-solvent in the RM "water pool" based on MeOH/H2O was investigated. We successfully found that MDL readily dissolved and showed an increased stability in MeOH/D2O mixtures ranging from 70% methanol to 90% methanol. Because MeOD is known to also form RMs using AOT/isooctane,41,42 we chose to use the mixtures with high concentrations of MeOD for better comparison with previous studies. 1D NMR studies were recorded of MDL in MeOD/D₂O mixture of AOT/isooctane. The fact that the chemical shifts of the observed protons in RMs differ from the chemical shifts of those in isooctane and MeOD/D₂O shows that the probe molecules are neither in the aqueous center or the organic outer layer; this is evidence of the probe molecules being the very least associated with the interface of the RMs (Fig. 10). As no changes were observed in the NMR spectra as the w_0 changed (data not shown), we concluded that the MDL penetrated or associated with the interface in these MeOD/D₂O/AOT/isooctane systems. As with the aqueous stability experiments, UV-vis spectra were recorded of NMR samples prepared from solid MDL added to the NMR tube before the MeOD/D₂O AOT RMs solution was added, allowing for the MDL to dissolve and move to interact with the RM suspen-

To obtain information on the location of the MDL, we performed 2D NMR NOESY and ROESY spectra using the w_0 16 sample in 70:30 MeOD/D₂O mixture, shown in Fig. 12. The oxidation of MDL took place while the 2D NMR NOESY and ROESY spectra were recorded. As a result, the spectra recorded show a mixture of the MEN and MDL and the amount of MDL present depends on when the spectrum was recorded. Similar studies were performed with the 90:10 and 70:30 mixtures and these spectra gave similar patterns.

In Fig. 12, there is an interaction between the internal control of $H_{e'}$ and $H_{x'}$ which shows that an NMR of MDL was obtained, but the lack of other cross peaks in the NMRs makes it difficult to determine the placement within the RM. It may be associated with the water pool, but the time span of the studies combined with the rate of oxidation of the MDL should be sufficient to observe cross peaks if there was an interaction. These results are consistent with an interaction with the interface for MEN. However, no firm conclusions can be made on the location of MDL in the RM system.

3.4.3. Benzoquinone (BEN) in microemulsions

To investigate the similarity of the interactions of 2,3-dimethoxy-5-methyl-1,4-benzoquinone (BEN), the headgroup of ubiquinone,

with a model membrane interface, ^1H NMR spectra were recorded in 0.50 mol/L AOT/isooctane (Fig. 13). The w_0 sizes were varied from w_0 4 to w_0 20. The 1D ^1H NMR spectra show that the chemical shifts for BEN are very different from those observed in isooctane and in D₂O (Figs. 13A and 13B). These shifts are consistent with BEN residing in neither the aqueous environment of the water pool, nor the organic isooctane solution, suggesting placement in the interface of the AOT RM. There is a small chemical shift change for H_a as the w_0 changes from 4 to 20. That is consistent with the fact that the BEN is located more in the Stern layer of the interface, placing it closer to the water pool than the tail region of interface.

To obtain confirmation regarding the location of BEN at the aqueous part of the interface, we performed $^1\mathrm{H}$ - $^1\mathrm{H}$ 2D NOESY and ROESY NMR (400 MHz) spectra of BEN inside w_0 12 RM at 26 °C (Figs. 13C and 13D). The partial $^1\mathrm{H}$ - $^1\mathrm{H}$ 2D NOESY spectrum of BEN inside w_0 12 RM show an interaction between $\mathrm{H_a}$ with the CH $_2$ groups in the AOT consistent with penetration of BEN into the interface. The partial $^1\mathrm{H}$ - $^1\mathrm{H}$ 2D NMR ROESY NMR spectra in a w_0 12 RM (Fig. 13D) show this interaction, as well are some additional interactions between $\mathrm{H_a}$ and the AOT protons, confirming the penetration of BEN with the interface.

3.5. DLS

DLS confirmed that RMs were formed and that the slight increase in RM size with the addition of MEN or MDL is within experimental error and suggest that overall the presence of these compounds is not interfering with the formation of the RMs. Data are presented in Supplementary Table S1.

4. Discussion

MK is a very important electron transport donor and accepter for bacteria and particularly pathogens like the *Mycobacterium* family.^{6,11,43} Despite this importance, very little experimental data are available with regard to MK's location in the cell membrane and how it moves from one location to another. Some experimental and computational work has been carried out for ubiquinone.^{14,30,44} A few computational studies have been reported that mention MK.⁴⁵ We have recently investigated how truncated MK derivatives interact with interfaces using both Langmuir monolayers and microemulsions. Considering the hydrophobicity of these compounds, they will undoubtedly be associated with the interface, but experimental data, more details on the nature of this association, and how lipoquinones move in a

Fig. 12. Partial 1 H- 1 H 2D (A) NOESY and (B) ROESY NMR (500 MHz) spectra of MDL and MEN in a 70:30 MeOD/D₂O 0.5 mol/L AOT RM suspension at 26 $^{\circ}$ C. Blue intensity contours represented negative NOEs or ROEs and red intensity contours represent positive NOEs or ROEs. A standard NOESY pulse consisted of 256 transients with 16 scans in the f_1 domain using a 200 ms mixing time and a 1.5 s relaxation delay. A standard ROESYAD pulse consisted of 256 transients with 16 scans in the f_1 domain using a 200 ms mixing time and a 2.0 s relaxation delay. [Colour online.]

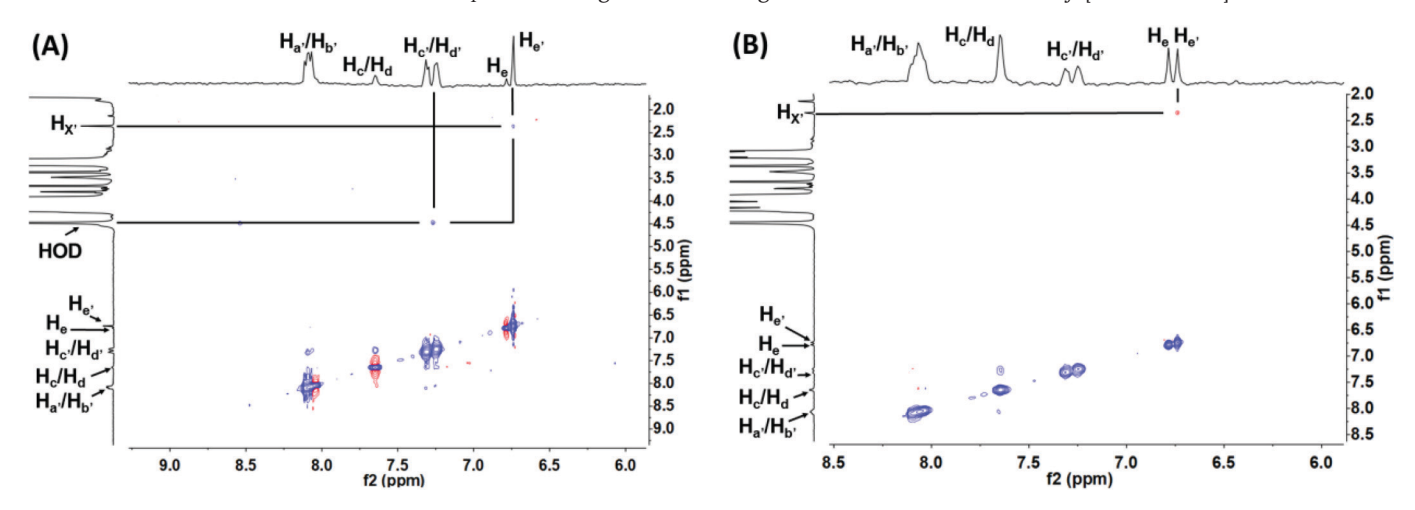
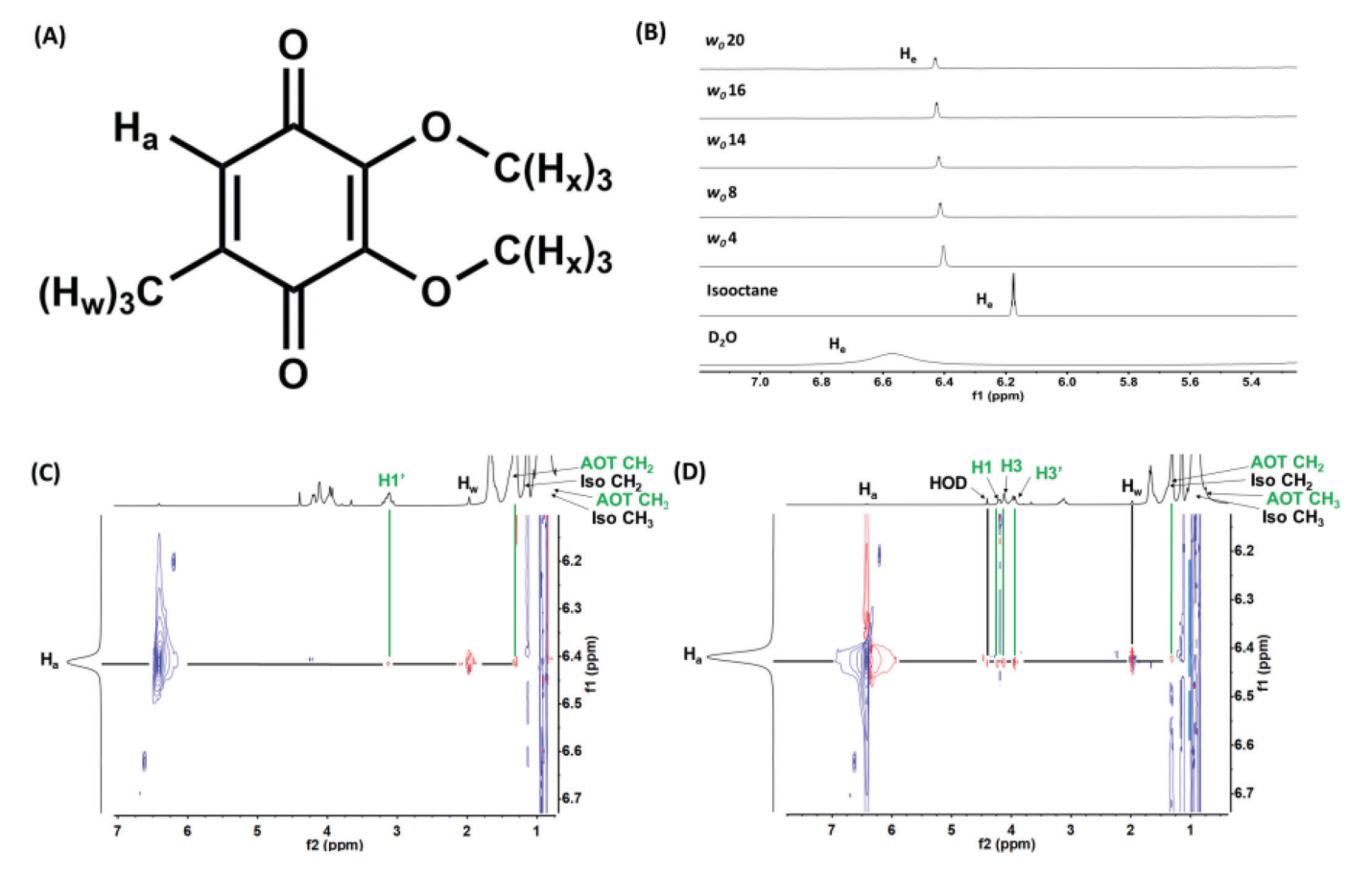


Fig. 13. (A) Structure with proton assignments of BEN. (B) 1D NMR of BEN in varying sizes of RM demonstrating that BEN is in the interface. Partial 1 H- 1 H 2D (C) NOESY and (D) ROESY NMR (400 MHz) spectra of BEN inside w_0 12 RM at 26 $^{\circ}$ C. Blue intensity contours represented negative NOEs or ROEs and red intensity contours represent positive NOEs or ROEs. A standard NOESY pulse consisted of 256 transients with 16 scans in the f_1 domain using a 200 ms mixing time and a 1.5 s relaxation delay. A standard ROESYAD pulse consisted of 256 transients with 16 scans in the f_1 domain using a 200 ms mixing time and a 1.5 s relaxation delay. Blue lines indicate BEN proton interactions with AOT protons. [Colour online.]



lipid environment are important for future understanding of electron transfer systems.

Lipoquinones are known to shuttle electrons within cell membranes, which requires these molecules to cycle between two redox states to function. In the oxidized form, lipoquinones have a

quinone headgroup, whereas the reduced form has a quinol headgroup. Quinones and quinols have different polarities, making it likely that they reside in different locations within the membrane. Current thought, however, favors the isoprenyl sidechain of a lipoquinone as the main determinant of location and inter-

action within the membrane.³⁰ For lipoquinones with the larger headgroup such as in menaquinones, it is possible that the headgroup plays a greater role than in ubiquinones. The studies in this manuscript investigate the association of MEN and MDL with two model interfaces. We anticipated that the difference in physical properties would be translated to differences in interaction and location of the compounds in the membrane bilayer.

Both MEN and MDL are hydrophobic and insoluble compounds. One may have anticipated that MDL would be more soluble than MEN because of the two hydroxyl groups. The fact that the MDL takes longer to dissolve than MEN is not consistent with this observation (see experimental section); furthermore, MDL only dissolved to higher concentrations when it oxidized to MEN. Generally, hydroxyl groups increase water solubility due to the increased polarity and the potential for H-bonding; however, this is not always the case as reported previously with, for example, the $[\mathrm{VO}_2(\mathrm{dipic}\mathrm{-OH})]^-$ and $[\mathrm{VO}_2\mathrm{dipic}]^-$ complexes. Thus, spectroscopic studies for MDL were limited by rapid oxidation despite being synthesized in pure form. The most convincing MDL data were obtained in the presence of reductant or in a stabilizing organic solvent such as MeOD.

The effects of MEN on a Langmuir monolayer were investigated using both DPPE and DPPC in Langmuir monolayers to properly characterize the interaction with different lipid interfaces. These lipids differ only in headgroup, where the choline headgroup of DPPC is a quaternary amine and the ethanolamine headgroup of DPPE is a primary amine. The different properties of these amine headgroups allow these phospholipids to fill different niches. The bulkier choline group allows for greater spreading of DPPC in conjunction with its fully saturated acyl tails, making it an ideal pulmonary surfactant.39 The smaller ethanolamine headgroup allows for tighter packing of DPPE, which is why it is more commonly found in the inner leaflet of the cell membrane.37,38 Our studies revealed a difference in the interaction of MEN with DPPC and DPPE. The DPPC compression isotherms showed no interaction. This implies that MEN either resides in the water or father up into the acyl tails and thus not in the interface. The DPPE studies showed a greater area per phospholipid as the amount of MEN increased. This is consistent with MEN remaining in the interface and disrupting the packing of the ethanolamine headgroups. This is analogous to studies of idebenone and idebenol, which were found to remain in the interface.33 Our studies also confirm that the lipid environment impacts the location and interaction of MEN in model membranes.40

Despite the difficulties in spectroscopic investigation of the MEN/MDL pair caused by the instability of MDL, studies were completed. We found that MEN interacted with the lipids and was able to penetrate the interface. Indeed, the isolated headgroup was found to reside in the tail ends of the interface. The NMR studies in the microemulsion model system supported the findings from the Langmuir monolayers with regard to the localization of the isolated headgroup. Studies with the MDL were more challenging and not as clean. Although conditions were found that allowed for characterization of the interactions of MDL with the reverse micellar interface, the 2D NMR results showed no evidence for penetration of the MDL into the interface. In contrast, results showed evidence for interactions with the HOD signal. However, 1D 1H NMR data did show that the MDL was not in an environment akin to aqueous or organic solvent, which suggests a location at the interface. With these two pieces of evidence combined, we suggest that the MDL is located at the interface near the water pool, although if and how deep the molecule penetrated could not be confirmed. Importantly, these results must be considered in the context of the full MK structure, where the isoprenyl sidechain will impact the properties of the quinone/quinol pair.

We have recently shown that the truncated MK derivatives, MK-1 and MK-2, adopt a folded conformation observed near the model AOT/RM membrane interface.^{1,13} Such a folded conforma-

tion would impact the location of the molecule. However, it is clear from these studies that the headgroup has the ability to direct the location of the lipoquinone, which in turn affects the action of these electron carriers and their travels between protein complexes within the membrane. Undoubtedly, structural and polarity differences in the lipoquinone headgroups contribute to different redox potentials, but perhaps less recognized is the fact that these differences may also aid in shuttling of these essential electron transport lipids in the membrane, aiding their function.

We were able to obtain experimental evidence that MEN is associated with the interface, likely through interactions with the AOT tail groups. This may be differentiated from headgroups of other lipoquinones such as BEN, the headgroup of ubiquinone. Additional NOESY and ROESY of BEN were collected under similar conditions to MEN as described in this manuscript. Spectra of BEN are shown in Fig. 13, and we observe interactions between H_a and the AOT protons found in the headgroup (H1, H1', H3, H3'), as well as the water pool. Comparing the two quinones, this implies that there are several factors in lipoquinone structure that may affect the location in the interface. Although we do not have data on the benzoquinol headgroup, it is likely that it would be located in a more polar environment, similar to both MDL and BEN. Previous studies with quinone/quinol pairs found that both molecules remained at the lipid-water interface.33 However, we cannot identify an exact location of MDL at the water-lipid interface. Further studies on compounds with quinol headgroups are desirable.

Interestingly, but not unexpectedly, MEN is located father up in the hydrophobic tail region than BEN considering that MEN is significantly more hydrophobic than BEN. Computational studies have found ubiquinone low in the tail region, nearer the water interface, which is consistent with the interactions of the head groups of AOT observed in the spectrum shown in Fig. 13.⁴⁶ These findings suggest that both the isoprenyl sidechain and the head-group will influence the location of lipoquinones.

In summary, the studies presented here show subtle differences in the location of the isolated headgroup MEN and MDL and subtle differences in the location of the isolated headgroup BEN compared with MEN in two types of model membranes, Langmuir monolayers and microemulsions. These studies provide experimental evidence that would be important to understand the location of menaquinones and menaquinols in membranes and their potential movement between membrane-bound protein complexes.

5. Conclusions

Based on structural considerations, it would not be unreasonable to expect that the MEN and MDL would occupy different locations in a membrane interface. Computational studies have been reported supporting the interpretation that lipoquinones change location in the membrane during the electron transfer process.46 These studies also have demonstrated that the isoprenyl side chain is important for this process. We investigated the interactions and locations of the headgroups of these compounds, namely MEN and MDL, with two model membrane interface systems. We found that MEN associates with the lipid tails. The MDL system was readily oxidized, precluding any Langmuir monolayer studies. However, NMR studies of MDL in microemulsions suggest a location in the water-lipid interface, albeit no exact location was identified. Considering that these studies are of isolated headgroups, this work suggests that the headgroup, in conjunction with the isoprenyl sidechain, is important for the location and interaction of lipoquinones with the cell membrane.

Supplementary data

Supplementary data are available with the article through the journal Web site at http://nrcresearchpress.com/doi/suppl/10.1139/cjc-2020-0024.

Acknowledgements

DCC and DCC thank NSF for partial funding (CHE-1709564). DCC and PM thank the NSF REU program for summer funding to PM (CHE-1461040).

References

- (1) Koehn, J. T.; Magallanes, E. S.; Peters, B. J.; Beuning, C. N.; Haase, A. A.; Zhu, M. J.; Rithner, C. D.; Crick, D. C.; Crans, D. C. J. Org. Chem. 2018, 83, 275. doi:10.1021/acs.joc.7b02649.
- Nowicka, B.; Kruk, J. Biochim. Biophys. Acta 2012, 1797, 1587. doi:10.1016/j bbabio.2010.06.007
- Das, A.; Hugenholtz, J.; van Halbeek, H.; Ljungdahl, L. G. J. Bacteriol. 1989, 171 (11), 5823. doi:10.1128/JB.171.11.5823-5829.1989
- Collins, M. D., Analysis of isoprenoid quinones. In: G. Gottschalk, editor. Methods in Microbiology. 1st ed. Academic Press, 1985; Vol. 18, pp. 329–366.
- (5) Dhiman, R. K.; Pujari, V.; Kincaid, J. M.; Ikeh, M. A.; Parish, T.; Crick, D. C. PLoS One 2019, 14 (4), e0214958. doi:10.1371/journal.pone.
- Upadhyay, A.; Kumar, S.; Rooker, S. A.; Koehn, J. T.; Crans, D. C.; McNeil, M. R.; Lott, J. S.; Crick, D. C. ACS Chem. Biol. 2018, 13 (9), 2498. doi:10.1021/acschembio.8b00402
- Schwalfenberg, G. K. J. Nutr. Metab. 2017, 2017, article 6254836. doi:10.1155/ 2017/6254836.
- Josey, B. J.; Inks, E. S.; Wen, X.; Chou, C. J. J. Med. Chem. 2013, 56 (3), 1007. doi:10.1021/jm301485d.
- Rahn, J. J.; Bestman, J. E.; Josey, B. J.; Inks, E. S.; Stackley, K. D.; Rogers, C. E.; Chou, C. J.; Chan, S. S. L. Neuroscience 2014, 259, 142. doi:10.1016/j.neuroscience.
- (10) Chadar, D.; Camilles, M.; Patil, R.; Khan, A.; Weyhermüller, T.; Salunke-Gawali, S. J. Mol. Struct. 2015, 1086, 179. doi:10.1016/j.molstruc.2015.01.029.
- (11) Upadhyay, A.; Fontes, F. L.; Gonzalez-Juarrero, M.; McNeil, M. R.; Crans, D. C.; Jackson, M.; Crick, D. C. ACS Cent. Sci. 2015, 1 (6), 292. doi:10. 1021/acscentsci.5b00212.
- (12) Kurosu, M.; Begari, E. Molecules 2010, 15, 1531. doi:10.3390/ molecules15031531.
- (13) Koehn, J. T.; Beuning, C. N.; Peters, B. J.; Dellinger, S. K.; Van Cleave, C.; Crick, D. C.; Crans, D. C. Biochemistry 2019, 58 (12), 1596. doi:10.1021/acs. biochem.9b00007.
- (14) Kaurola, P.; Sharma, V.; Vonk, A.; Vattulainen, I.; Róg, T. Biochim. Biophys. Acta 2016, 1858 (9), 2116. doi:10.1016/j.bbamem.2016.06.016.
- (15) Quinn, P. J.; Esfahani, M. A. Biochem. J. 1980, 185 (3), 715. doi:10.1042/ bi1850715.
- (16) Roche, Y.; Peretti, P.; Bernard, S. J. Therm. Anal. Calorim. 2007, 89, 867. doi: 10.1007/s10973-006-7916-4.
- (17) Möhwald, H.; Brezesinski, G. Langmuir 2016, 32 (14), 10445. doi:10.1021/acs. langmuir.6b02518
- Peters, B. J.; Van Cleave, C.; Haase, A. A.; Hough, J. P. B.; Giffen-Kent, K. A.; Cardiff, G. M.; Sostarecz, A. G.; Crick, D. C.; Crans, D. C. Langmuir 2018, 34 (30), 8939. doi:10.1021/acs.langmuir.8b01661.
- (19) Eskici, G.; Axelsen, P. H. J. Phys. Chem. B 2016, 120 (44), 11337. doi:10.1021/acs. jpcb.6b06420.
- (20) Crans, D. C.; Rithner, C. D.; Baruah, B.; Gourley, B. L.; Levinger, N. E. J. Am. Chem. Soc. 2006, 128 (13), 4437. doi:10.1021/ja0583721.

- (21) Koehn, J. T.; Crick, D. C.; Crans, D. C. ACS Omega 2018, 3 (11), 14889. doi:10. 1021/acsomega.8b02620
- (22) Wiebenga-Sanford, B. P.; Washington, J. B.; Cosgrove, B.; Palomares, E. F.; Vasquez, D. A.; Rithner, C. D.; Levinger, N. E. J. Phys. Chem. B 2018, 122, 9555. doi:10.1021/acs.jpcb.8b07406
- (23) Correa, N. M.; Silber, J. J.; Riter, R. E.; Levinger, N. E. Chem. Rev. 2012, 112, 4569. doi:10.1021/cr200254q.
- (24) Maitra, A. J. Phys. Chem. 1984, 88 (21), 5122. doi:10.1021/j150665a064
- (25) Binks, B. P.; Meunier, J.; Abillon, O.; Langevin, D. Langmuir 1989, 5 (2), 415. doi:10.1021/la00086a022.
- (26) Mukherjee, K.; Mukherjee, D. C.; Moulik, S. P. J. Colloid Interface Sci. 1997, 187 (2), 327. doi:10.1006/jcis.1996.4696.
- (27) Van Horn, W. D.; Oglivie, M. E.; Flynn, P. F. J. Biomol. NMR 2008, 40 (3), 203. doi:10.1007/s10858-008-9227-5.
- (28) Sostarecz, A. G.; Gaidamauskas, E.; Distin, S.; Bonetti, S. J.; Levinger, N. E.;
- Crans, D. C. *Chemistry* **2014**, *20* (17), 5149. doi:10.1002/chem.201201803. (29) Peters, B. J.; Groninger, A. S.; Fontes, F. L.; Crick, D. C.; Crans, D. C. *Langmuir* 2016, 32 (37), 9451. doi:10.1021/acs.langmuir.6b02073.
- (30) Teixeira, M. H.; Arantes, G. M. RSC Adv. **2019**, 9, 16892. doi:10.1039/ C9RA01681C
- (31) Monteiro, J. P.; Martins, A. F.; Nunes, C.; Morais, C. M.; Lúcio, M.; Reis, S.; Pinheiro, T. J. T.; Geraldes, C. F. G. C.; Oliveira, P. J.; Jurado, A. S. *Biochim.* Biophys. Acta 2013, 1828, 1899. doi:10.1016/j.bbamem.2013.04.006.
- (32) Ausili, A.; Torrecillas, A.; de Godos, A. M.; Corbalán-García, S.; Gómez-Fernández, J. C. Langmuir 2018, 34 (10), 3336. doi:10.1021/acs.langmuir.
- (33) Gómez-Murcia, V.; Torrecillas, A.; de Godos, A. M.; Corbalán-García, S.; Gómez-Fernádez, J. C. Biochim. Biophys. Acta 2016, 1858, 1071. doi:10.1016/j. bbamem.2016.02.034.
- (34) Suhara, Y.; Wada, A.; Tachibana, Y.; Watanabe, M.; Nakamura, K.; Nakagawa, K.; Okano, T. Bioorg. Med. Chem. 2010, 18 (9), 3116. doi:10.1016/j. bmc.2010.03.035.
- (35) Stahla, M. L.; Baruah, B.; James, D. M.; Johnson, M. D.; Levinger, N. E.; Crans, D. C. Langmuir 2008, 24 (12), 6027. doi:10.1021/la8002965.
- (36) Yang, L.; la Cour, A.; Anderson, O. P.; Crans, D. C. Inorg. Chem. 2002, 41, 6322. doi:10.1021/ic0201598
- (37) Patterson, M.; Vogel, H. J.; Prenner, E. J. Biochim. Biophys. Acta 2016, 1858, 403. doi:10.1016/j.bbamem.2015.11.025.
- (38) Fadeel, B.; Xue, D. Crit. Rev. Biochem. Mol. Biol. 2009, 44 (5), 264. doi:10.1080/ 10409230903193307
- (39) Al-Saiedy, M.; Tarokh, A.; Nelson, S.; Hossini, K.; Green, F.; Ling, C.-C.; Prenner, E. J.; Amrein, M. Biochim. Biophys. Acta 2017, 1859 (8), 1372. doi:10. 1016/j.bbamem.2017.05.004.
- (40) Baryiames, C. P.; Teel, M.; Baiz, C. R. Langmuir 2019, 35, 11463. doi:10.1021/ acs.langmuir.9b01693.
- Lu, R.; Zhu, R.; Zhong, R.; Yu, A. J. Photochem. Photobiol. A 2013, 252, 116. doi:10.1016/j.jphotochem.2012.12.004.
- (42) Shirota, H.; Horie, K. J. Phys. Chem. B 1999, 103 (9), 1437. doi:10.1021/
- (43) Dhiman, R. K.; Mahapatra, S.; Slayden, R. A.; Boyne, M. E.; Lenaerts, A.; Hinshaw, J. C.; Angala, S. K.; Chatterjee, D.; Biswas, K.; Narayanasamy, P., et al. Mol. Microbiol. 2009, 72 (1), 85. doi:10.1111/j.1365-2958.2009.06625.x.
- (44) Hoyo, J.; Guaus, E.; Torrent-Burgués, J. Eur. Phys. J. E: Soft Matter Biol. Phys. 2017, 40 (62), 62. doi:10.1140/epje/i2017-11552-2.
- (45) Chatron, N.; Hammed, A.; Benoît, E.; Lattard, V. Nutrients 2019, 11, 67. doi: 10.3390/nu11010067.
- (46) Galassi, V. V.; Arantes, G. M. Biochim. Biophys. Acta 2015, 1847, 1560. doi:10. 1016/j.bbabio.2015.08.001.